Active Noise Cancellation in Headphones by Digital Robust Feedback Control

Stefan Liebich, Carlotta Anemüller, Peter Vary, Peter Jax
Institute for Communication Systems
RWTH Aachen University
Email: {liebich,anemueller,vary,jax}@iks.rwth-aachen.de

Daniel Rüschen, Steffen Leonhardt
Philips Chair for Medical Information Technology
RWTH Aachen University
Email: {rueschen,leonhardt}@hia.rwth-aachen.de

***Abstract*—Active Noise Cancellation (ANC) may complement passive insulation of headphones by actively cancelling low frequency components of acoustical background noise. In systems with a single error microphone pointing towards the ear canal, a feedback controller performs the compensation task. We are focusing on fixed feedback controllers for broadband attenuation of arbitrary ambient noise.**

We use methods and optimization routines from control theory. In this discipline the key element is the so-called controller, which is in terms of signal processing a (digital) filter.

The controller is designed by an optimization approach called the mixed-sensitivity $\mathcal{H}_\infty$ synthesis, which requires an accurate estimate of the secondary path between the cancelling loudspeaker and the error microphone, and the knowledge of the secondary path uncertainties as well as a specification of the closed-loop sensitivity. The advantage of this method is the convenient formulation of performance and uncertainty requirements in the frequency domain. We describe the design process and evaluate the controller, which is realized in state space form, within a real-time system.

The real-time measurements show a good match with the expected behavior. They furthermore confirm the feasibility of broadband attenuation by fixed i.e. time invariant feedback controllers in a digital system.

The novelty of this contribution comprises of the specific design process of a discrete robust feedback controller for broadband noise reduction (roughly $250\,$Hz) and the digital real-time system implementation.

I. Introduction

Acoustical noise pollution is a major subjective disturbance e.g. in airplanes, at contruction sites as well as in industrial and production plants. Headphones with a combined passive noise attenuation and active noise cancellation (ANC) offer a promising solution, as they complement each other very well in their frequency dependent insulation.

The technological advances of digital signal processors and low latency analog-to-digital converters (ADC) and digital-to-analog converters (DAC), allow for digital ANC implementations. Within this research field, *adaptive* feedforward and feedback systems dominate [1].

The system inherently incorporates a latency between the acquisition of the noise and the radiation of a cancelling signal. Considering this limitation, the known *digital adaptive feedback systems* may only cancel deterministic and periodic signals. *Fixed feedback controllers* on the other hand have shown to be able to attenuate disturbances with a constant characteristic in analog systems [2]. We are focusing on the investigation of *digital fixed feedback controllers*.

Various methods for designing such controllers require manual and heuristical constructions (e.g. PID, internal mode controller, loop shaping [3]). The performance of such manually designed feedback controllers is mostly far from optimal. Furthermore, they offer only an unstructured handling of path uncertainties [3]. Though the stability of the controller in varying circumstances connected with uncertainties of the system is one of the major objectives in ANC headphones. Uncertainty originates e.g. from different headphone positions, enclosed volume, material of the earpiece, etc.

A more promising approach is the so-called mixed-sensitivity $\mathcal{H}_\infty$ control method. It optimizes the $\mathcal{H}_\infty$ norm of sensitivity functions and includes frequency dependent model uncertainty. The basic idea of the $\mathcal{H}_\infty$ synthesis was first proposed by Zames in 1979 [4]. In the following two decades, efficient solutions of the mathematical $\mathcal{H}_\infty$ problem became available (see e.g. [5], [6]). The approach mainly originates from controller design for analog circuits (e.g. [2] in ANC headphones).

$\mathcal{H}_\infty$ synthesis for digital systems has already been used for some acoustical applications. E.g. in [7], the mixed-sensitivity $\mathcal{H}_\infty$ synthesis was applied to a one-dimensional acoustic duct. Narrowband noise was considered and very small attenuation bandwidths of $10\,$Hz was achieved.

In contrast to the aforementioned publications, we are aiming for a digital real-time implementation with broadband attenuation. The novelty of this contribution is the combination of state-of-the-art acoustic measurement techniques, the modeling approaches as well as the specific mixed-sensitivity $\mathcal{H}_\infty$ controller synthesis and implementation of a discrete controller.

II. The problem

Fig. 1 illustrates the functional structure of an ANC headphone. In addition to the loudspeaker, it contains an error microphone for capturing the acoustic signal within the ear canal.

The ambient noise signal $x'(t)$[1] is passively attenuated by the headphone and perceived as $d'(t)$[2] within the ear

[1]For simplicity we use the same names for discrete time k and continuous time t variables e.g. $e(t)$ and $e(k) = e(kT)$ or $G(s) = \mathscr{L}\{g(t)\}$ and $G(z) = \mathscr{Z}\{g(k)\}$, whereas $z = e^{sT}$.

[2]The symbol $'$ indicates the acoustical representation of the signals.

978-0-9928-6265-7/16/$31.00 ©2016 IEEE

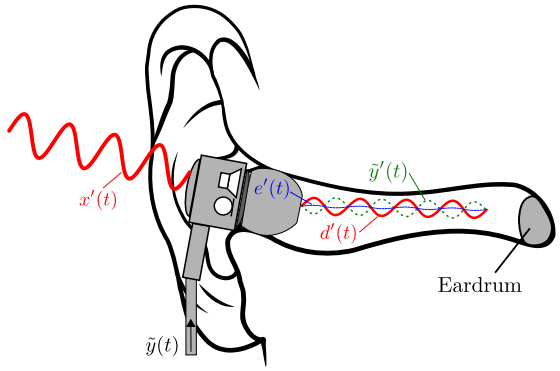

Fig. 1. Functional structure of the ANC in-ear headphone and the corresponding sound signals.

canal. To cancel this disturbance the controller is creating a cancellation signal $\tilde{y}'(t)$, which interferes with $d'(t)$ and leaves the acoustical error signal $e'(t)$.

A system model including the so-called secondary path $G(z)$, the controller $K(z)$ and the secondary path estimate $\hat{G}(z)$ is shown in Fig. 2.

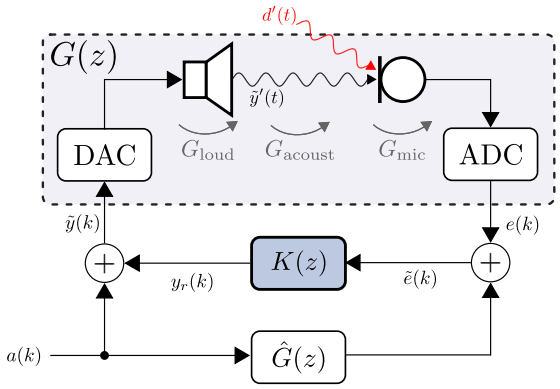

Fig. 2. Components of the secondary path G with the feedback controller K and an optional audio signal $a(k)$.

The secondary path G describes the transfer between the loudspeaker output $\tilde{y}(k)$ and the microphone input $e(k)$ of the digital system. It contains the DAC, the loudspeaker characteristic G_{loud}, the acoustic transmission G_{acoust}, the microphone characteristic G_{mic} and the ADC. The secondary path represents the path to be controlled. The controller $K(z)$ is creating a cancellation signal $\tilde{y}'(t)$, which attenuates the disturbance $d'(t)$. Parallel to the control loop an audio signal $a(k)$ can be added to the controller output $y_r(k)$. Under the realistic assumption of a sufficiently accurate estimate $\hat{G}(z)$ of the secondary path, this component needs not to be considered for the ANC task.

III. Mixed-Sensitivity $\mathcal{H}_\infty$ Optimization

A common approach for designing a controller is mixed-sensitivity $\mathcal{H}_\infty$ synthesis, in which the closed loop sensitivity functions are directly shaped by solving an optimization problem [3]. It allows the incorporation of uncertainty in the control design process. Fig. 3 illustrates the augmented plant,

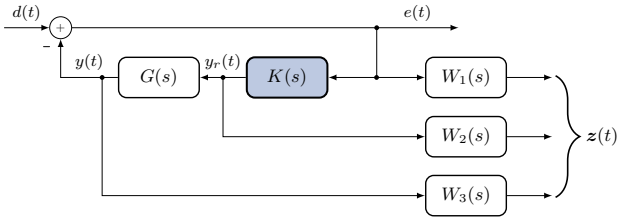

Fig. 3. Feedback Control System with mixed-sensitivity weighting functions W_1 to W_3 without additional audio signal.

which is the base for the optimization routine. The weighting functions W_i with $i \in \{1, 2, 3\}$, contain the design goals and can be interpreted as cost functions over frequency.

For the formulation of the objective function we are furthermore considering the *sensitivity function*

$$S(s) = \frac{1}{1 + G(s)K(s)}, \tag{1}$$

which is the transfer function from the disturbance d to the control error e. It quantifies the sensitivity to output disturbance and small parameter variations. The *complementary sensitivity function*

$$T(s) = \frac{G(s)K(s)}{1 + G(s)K(s)} \tag{2}$$

describes the response to measurement noise n, which assumed to be insignificant and therefore not shown in Fig. 3. The terminology originate from the identity

$$S(s) + T(s) = 1, \tag{3}$$

which holds for all frequencies. The control error for a general regulation problem is given by

$$E(s) = S(s)D(s) - T(s)N(s). \tag{4}$$

Ideally, S should be small to reject the disturbance d and T should be small to lower the sensitivity against measurement noise n. As this is impossible to achieve simultaneously, Eq. (3) is sometimes referred to as "fundamental dilemma" of control.

The controller K presented in this paper was designed with mixed-sensitivity $\mathcal{H}_\infty$ optimization using the objective function

$$\min_K \left\| \boldsymbol{T}_{zd}(s) \right\|_\infty \tag{5}$$

with

$$\left\| \boldsymbol{T}_{zd}(s) \right\|_\infty = \left\| \begin{bmatrix} W_1(s)S(s) \\ W_2(s)K(s)S(s) \\ W_3(s)T(s) \end{bmatrix} \right\|_\infty = \gamma \tag{6}$$

where all entries are single input single output transfer functions in the Laplace domain. The corresponding augmented plant is illustrated in Fig. 3.

The $\mathcal{H}_\infty$ norm is defined as the peak absolute value of the maximum singular value as follows.

$$\left\| \boldsymbol{T}_{zd}(s) \right\|_\infty = \sup_\omega \bar{\sigma}\left(\boldsymbol{T}_{zd}(j\omega) \right) \tag{7}$$

The maximum singular value is the square root of the maximum of the eigenvalues $\lambda_i = \text{eig}(\boldsymbol{T}_{zd}^H \boldsymbol{T}_{zd})$, with $\boldsymbol{T}_{zd}^H$ being the complex conjugate transpose of $\boldsymbol{T}_{zd}$:

$$\bar{\sigma}(\boldsymbol{T}_{zd}) = \sqrt{\max_i(\lambda_i)}. \tag{8}$$

For single input, single output systems $\boldsymbol{T}_{zd}$ is a vector and $\bar{\sigma}(\boldsymbol{T}_{zd})$ reduces to the Euclidean vector norm [3].

The control designer can affect the solution of the mixed-sensitivity synthesis by choosing the weighting functions W_i included in Eq. (6). They must be proper and stable. Hence, W_1 is usually a low-pass filter with approximately the same bandwidth as the disturbance signal. The weighting W_2 penalizes control action and is of lesser importance in signal processing applications. Therefore, it is neglected and set to 0 in the design process. W_3 is often implemented as a high-pass filter with a cross-over frequency at the desired closed loop bandwidth.

Unfortunately, it is not possible to shape the sensitivity functions arbitrarily. One limitation is given by Bode's sensitivity integral [8], also known as the waterbed effect. In case the stable open loop transfer function $G \cdot K$ has a pole excess of at least two, then for closed-loop stability the sensitivity function has to satisfy

$$\int_0^\infty \ln|S(j\omega)| \mathrm{d}\omega = 0. \tag{9}$$

Eq. (9) implies that the reduction of sensitivity in one frequency range entails a sensitivity increase in another.

Although robust control methods can not overcome the limitations imposed by inherent path properties, the controllers synthesized are robustly stable within these limitations. The main benefit of mixed-sensitivity $\mathcal{H}_\infty$ control is the possibility to describe performance specifications directly in the frequency domain, which is very convenient for ANC.

IV. Controller/Filter Design for ANC Headphones

For all follorwing illustrations we are regarding the dependency on the frequency $\omega = 2\pi f$. We therefore evaluate $s = j\omega = j2\pi f$ and $z = e^{j2\pi f/f_s}$.

A. Secondary Path Modeling

We have conducted acoustic measurements with logarithmic sweep signals [9] to measure a time-discrete secondary path $G_{\text{meas}}(z)$ model. The real system is analog by nature. Therefore, a representation of all paths in the Laplace domain is adequate. Furthermore, the utilized $\mathcal{H}_\infty$ optimization routines use a Laplace domain representation. Therefore, we derive a continuous model from the discrete data. It is of great importance that the magnitude as well as the phase of the secondary path are preserved.

In the first step we are estimating a transfer function model in the z-domain with the prediction error minimization method (PEM) to reduce the model order [10]. Thereafter, the continuous representation in the Laplace domain, is approximated by linear interpolation of the time discrete samples (first-order hold method).

The magnitude and the phase responses of the measurement and the measurement of the secondary path are shown in Fig. 4. Apart from slight overestimation of the magnitude at higher frequencies and a slight deviation between 300 and 1000 Hz the characteristics are very well sustained. The final model G(s) for the $\mathcal{H}_\infty$ optimization is a transfer function of order 16.

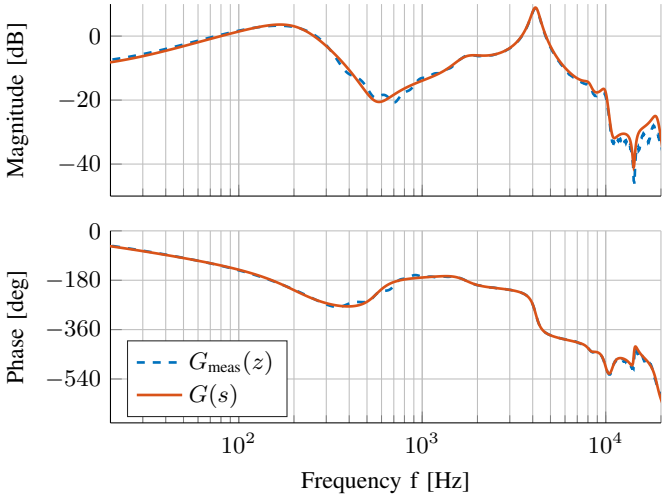

Fig. 4. The magnitude and phase response of the secondary path with both the discrete measurement $G_{\text{meas}}(z)$ and the model $G(s)$.

B. Modelling the Uncertainty

The system to be controlled is characterized by a certain amount of variation in its paths manifesting in an uncertainty. In the case of ANC headphones this includes the enclosed volume of the ear canal, the quality of the occlusion and the material of the ear piece.

We combine the various sources of uncertainty in the following multiplicative form [3].

$$G_{\text{p}}(s) = G(s) \cdot (1 + W_{\text{M}}(s)\, \triangle_{\text{I}}(s)) \;\text{ with }\; |\triangle_{\text{I}}(j\omega)| \leq 1 \forall \omega \tag{10}$$

The set of perturbed path models included in $G_{\text{p}}(s)$, contain all paths that lie within the range of upper boundary $W_{\text{M}}(s)$ around $G(s)$. This is realized by $\triangle_{\text{I}}(s)$, which describes any stable tranfer function with magnitude less than or equal 1 for all frequencies.

The goal is to design a controller which is stable in all practical situations. This may be expressed by the robust stability condition [3].

$$|T(j\omega)| < 1/|W_{\text{M}}(j\omega)|, \;\forall\omega \tag{11}$$

To cover all practical scenarios we measured typical use cases as well as extreme cases. This includes different positions of the headphone, as well as open ear use and complete covering of the ear piece. The transfer functions acquired of the different scenarios $G_{\text{scen}}(j\omega)$ may be condensed into a measured upper boundary $W_{\text{M}}(j\omega)$ by taking the maximum over all scenarios for each frequency.

$$|W_{\text{M}}(j\omega)| = \max_{G_{\text{scen}}} \left| \frac{G_{\text{scen}}(j\omega) - G(j\omega)}{G(j\omega)} \right|. \tag{12}$$

The weighting function W_3 may be chosen arbitrarily but should not decrease below W_{M}. We increased the uncertainty within W_3 for low frequencies below 30 Hz and for frequency above 10 kHz as shown in Fig. 5, due to the observed typical measurement inaccuracies of small electret microphone capsules. Furthermore, the uncertainty between 700 Hz and 10 kHz was raised in two steps as we wanted the controller to have a wide-spread amplification in the high frequency range.

As we are mostly interested in the magnitude response, it is suitable to assume a minimum-phase system for W_3. To accurately approximate the logarithmic magnitude response as a state space model we are using the log-Chebyshev magnitude design. Thereafter, this discrete model is converted into a continuous representation with the same method as the secondary path.

Fig. 5 illustrates the measured uncertainty bound $W_{\mathrm{M}}(s)$ as well as the continuous model of the modified uncertainty $W_3(s)$ in the frequency domain. W_3 has a model order of 20.

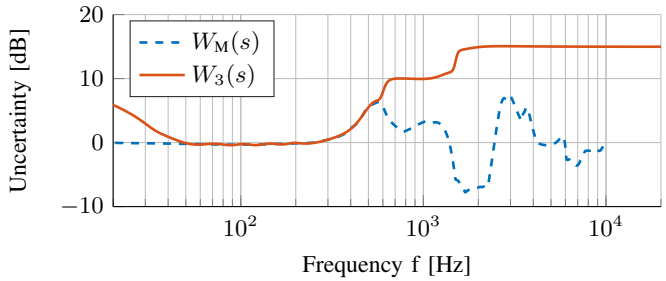

Fig. 5. Measured uncertainty $W_{\mathrm{M}}(s)$ and the continuous model of the modified uncertainty W_3.

C. Composition of the Sensitivity Bound

The controller shall accomplish broadband attenuation at low frequencies to complement the passive insulation of high frequencies of the headphone.

As described by Eq. (9), an attenuation of certain frequency bands always comes at the price of an amplification in other frequency bands. Therefore, we have to choose a trade-off between high attenuation, attenuation bandwidth and amplification. Due to Eq. (3), a high attenuation in frequency ranges with a high uncertainty is not possible if the controller has to remain stable.

Both limitations were considered when choosing the sensitivity bound $|W_1^{-1}|$, which is shown in the upper plot in Fig. 6. $|W_1^{-1}|$ crosses 0 dB at approximately 27 and 650 Hz, with a maximum attenuation of about 22 dB.

W_1 was modelled as a band-pass filter, which can be defined as the combination of a low- and a high-pass filter [3]. This manual modeling of the sensitivity bound resulted in model order of $m = 6$.

D. Controller Design, Model Reduction and Discretization

We use a state space approach based on the solution of two Riccati equations (ARE) proposed in [5] for solving the optimization problem and calculating a continuous controller.

A real world implementation of an ANC system always incorporates the burden of limited computational capabilities. Thus, the order of the controller $K(s)$ play in an important role in the design process. One method to reduce the order with as little influence as possible is based on Hankel singular values. The Hankel singular values of a system $K(s)$ basically represent the energy of each state, which corresponds to the input-output behaviour. For a detailed explanation it is referred to [3]. The $n - k$ states with the smallest Hankel singular values are neglected to create a reduced model K_{red}.

For the application of the controller in a real-time system we require a discrete time version $K(z)$. The conversion of the continuous time controller $K(s)$ is derived from the analytical solution of the describing differential state space equation. The input signal $e(t)$ was assumed as piecewise linear between adjacent samples $e(kT)$ (first-order/triangle hold equivalent) [11].

V. Evaluation

A. Controller Evaluation

The result of the previously described design process is a discrete controller of order 20 in state space form. The upper plot of Fig. 6 illustrates the sensitivity function S and thereby the closed loop characteristic for disturbance together with the design goal specified by $1/W_1$. The design specifications are not completely met, as

$$|S(j\omega)| < 1/|W_1(j\omega)| \tag{13}$$

is not fulfilled for all frequencies. Nevertheless, an attenuation of at least 10 dB is predicted for the frequency range from 70 to 325 Hz. Following the waterbed effect in Eq. (9) other frequency ranges are amplified as a price for the attenuation. We may observe an amplification of roughly 5 dB at very low frequencies below 30 Hz and an amplification of $1 - 2$ dB in a very wide frequency band above 1 kHz. This design results in a wide-spread amplification as desired.

The complementary sensitivity T together with the design goal $1/W_3$ and the measured uncertainty $1/W_{\mathrm{M}}$ is shown in the lower plot of Fig. 6. Again the design specifications have been a little too restrictive and

$$|T(j\omega)| < 1/|W_3(j\omega)| \tag{14}$$

was not met for all frequencies. However, for the closed-loop stability we have to consider the robust stability. We may observe that in the frequency range of 400 to 650 Hz the inequality (11) is not met. In this range the controller design is suffering from the dilemma of feedback control, presented in Eq. (3). We sacrificed stability to improve attenuation in the presence of uncertainty.

All requirements of the design are met by the controller if the parameter $\gamma < 1$ (cmp. Eq. (6)) Due to the observed deviations, the controller K achieved $\gamma = 2.3075$.

Very common performance parameters typically connected with feedback controllers are the gain margin GM and phase margin PM [3]. GM describes how much the gain can be increased and PM represents how high the phase lag may get before the closed loop system gets unstable. The controller K achieves $GM = 7.35$ dB and $PM = 71.2°$. Both have been

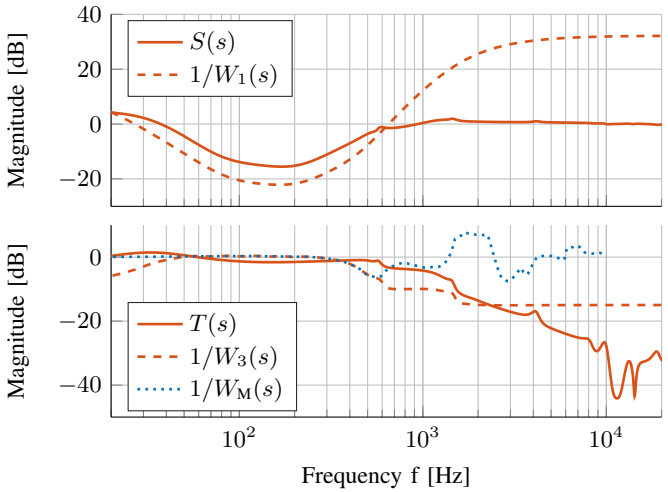

Fig. 6. Sensitivity S and the design target, the inverse weighting function W_1 (upper); Complementary sensitivity T, the design target given by the inverse weighting function W_3 and the measured uncertainty W_M (lower).

determined by utilizing the Nyquist diagram of the discrete system.

B. Real-Time Measurements

The real-time system was implemented with dSPACE hardware (DS1005, dSPACE GmbH, Paderborn, Germany), with the DS2004 AD-extension and the DS2102 DA-extension board. The round trip delay of this system, including the DAC and the ADC, but excluding the acoustics, is 1 sample at a sampling rate of $f_s = 48\,\text{kHz}$. We integrated a *Bose QC 20* headphone hardware (without the Bose ANC electronics) into our system. It contains a reference microphone for recording the outer sound signals, as well as an error microphone, for capturing the sound signals inside the ear canal [12]. All measurements were performed with a dummyhead (HMS II.3 with 6460 MFE VI amplifier, HEAD acoustics GmbH, Herzogenrath, Germany).

The fixed feedback controller shows a deterministic frequency behaviour independent of the input signal. We used a logarithmic sweep signal as the outer disturbance $x(t)$. For isolated consideration of the active noise cancellation part, we relate the magnitude spectra of the remaining sound without cancellation $d(t)$ and the error signal $e(t)$ with cancellation. The measurement $S_{\text{meas}}(z)$ and the predicted behaviour $S(s)$ are shown in Fig. 7. For acquiring the results, four measurements

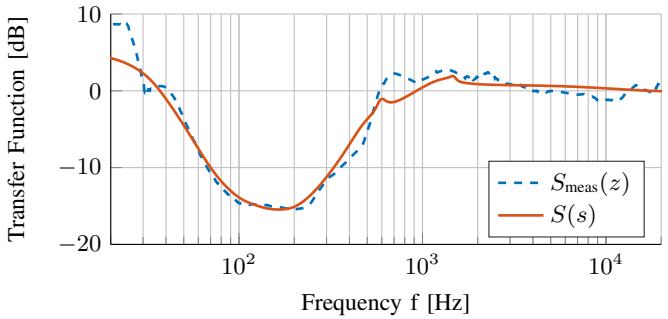

Fig. 7. Measured attenuation achieved by the fixed controller K.

of a $t_{\text{meas}} = 10\,\text{s}$ long logarithmic sweep have been averaged. The final transfer function $S_{\text{meas}}(z)$ has been smoothed with a 1/3-octave band average filter. Comparing the prediction and the measurement we observe a good agreement of the sensitivity $S(s)$ and the actual attenuation $S_{\text{meas}}(z)$. However, we also encounter a slight deviation from the predicted behaviour. There is an additional amplification for low frequencies below 30 Hz, which could be due to microphone limitations. Additionally the measurements show amplification in the range 600 Hz to 3 kHz. The slight deviations can be caused by a change of the secondary path $G(s)$, which occurs due to a different fitting position of the headphone.

VI. Conclusion

An ANC headphone with a fixed feedback controller has been implemented as a digital real-time system. The controller was designed using an approach from robust control theory, the mixed-sensitivity $\mathcal{H}_\infty$ synthesis, incorporating direct frequency domain representation of performance and stability requirements.

The performance requirements were chosen for attenuating frequencies in the range between 40 and 650 Hz. Within the real-time evaluations we confirmed the characteristics of the closed-loop sensitivity S. Due to the low delay of the secondary path, we achieve a broadband attenuation of at least 10 dB within the range of 70 to 325 Hz with a feedback ANC system. This is a significantly wider bandwidth than in previous publications with less or equal 10 Hz [7]. Furthermore, we distributed the amplification over a wide frequency range. The system amplifies roughly $1-2\,\text{dB}$ at frequencies above 1 kHz and roughly 5 dB below 30 Hz.

References

[1] S. Kuo and D. Morgan, "Active noise control: a tutorial review," *Proceedings of the IEEE*, vol. 87, no. 6, pp. 943–973, Jun 1999.
[2] M. Bai and D. Lee, "Implementation of an active headset by using the H robust control theory," *Acoustical Society of America Journal*, vol. 102, pp. 2184–2190, Oct. 1997.
[3] S. Skogestad and I. Postlethwaite, *Multivariable feedback control: analysis and design*. John Wiley & Sons, 2005.
[4] G. Zames, "Feedback and optimal sensitivity: model reference transformations, weighted seminorms, and approximate inverses," in *Proceedings of the 17th Allerton Conference*, 1979, pp. 744–752.
[5] J. Doyle, K. Glover, P. Khargonekar, and B. Francis, "State-space solutions to standard H_2 and H_∞ control problems," *IEEE Trans. Autom. Control*, vol. 34, no. 8, pp. 831–847, 1989.
[6] T. Iwasaki and R. E. Skelton, "All controllers for the general H_∞ control problem: LMI existence conditions and state space formulas," *Automatica*, vol. 30, no. 8, pp. 1307–1317, 1994.
[7] R. Sanchez Pena, M. Cuguero, A. Masip, J. Quevedo, and V. Puig, "Robust identification and feedback design: An active noise control case study," *Control Engineering Practice*, vol. 16, no. 11, pp. 1265–1274, 2008.
[8] K. Zhou, J. C. Doyle, and K. Glover, *Robust and optimal control*. Prentice Hall, 1996.
[9] S. Müller and P. Massarani, "Transfer-function measurement with sweeps," *J. Audio Eng. Soc*, vol. 49, no. 6, pp. 443–471, 2001.
[10] Soederstroem and Stoica, *System Identification*. Prentice Hall, 1989.
[11] G. F. Franklin, J. D. Powell, and M. L. Workman, *Digital control of dynamic systems*. Addison-wesley Menlo Park, 1998, vol. 3.
[12] K. Annunziato, J. Harlow, M. Monahan, A. Parthasarathi, R. Silvestri, and E. Wallace, "In-ear active noise reduction earphone," Patent US Patent 8,682,001, Mar. 25, 2014.